

Electron-optical properties of the Eindhoven race-track microtron

G.A. Webers, L.H.A. Leunissen, J.L. Delhez, J.I.M. Botman, H.L. Hagedoorn
Eindhoven University of Technology
P.O. Box 513, 5600 MB Eindhoven
The Netherlands

Abstract

The Eindhoven Race-track microtron contains two inhomogeneous bending magnets to obtain sufficient transverse focusing. For the design of these magnets we have used a first-order matrix theory to describe particle trajectories. Recently, higher-order terms of the magnetic field have been taken into account and the effects on the transverse motions have been studied. Here, we have used the numerical code COSY INFINITY [1] as well as numerical orbit integrations through the measured field maps.

1 INTRODUCTION

At Eindhoven University of Technology, a 75 MeV race-track microtron (RTME) [2] is being designed and constructed. This microtron (see Figure 1) will serve as injector for the electron storage ring EUTERPE [3]. The electrons are injected from a 10 MeV revised medical linac into the microtron and are accelerated in a 2998 MHz standing wave structure with an accelerating voltage of 5 MV. Combined-function magnets have been used to provide closed orbits as well as sufficient focusing forces [4]. Furthermore, the magnets have been rotated in their median planes to assure closed orbits. The profile of the magnet poles consists of two distinct sectors (sector I and II) such that the air gaps are 20 and 17 mm, respectively. The magnetic field in sector I and II are 0.51 T and 0.60 T, respectively. The distance on the cavity-axis between the bending magnets is 0.99 m. The main RTME parameters

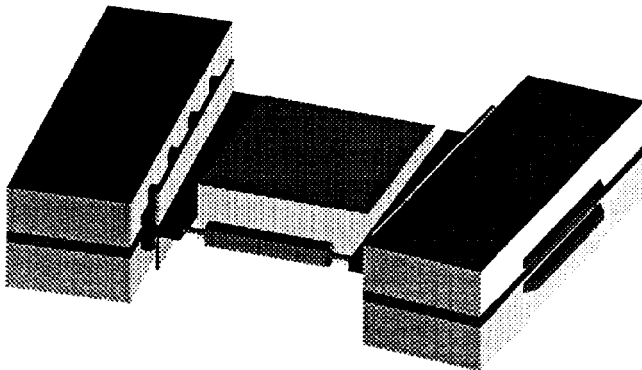


Figure 1: Perspective view of the Eindhoven race-track microtron

are listed in Table 1.

Table 1: Main RTME parameters.

RF frequency ($\lambda=0.10$ m)	2998 MHz
Magnet separation	0.99 m
Injection energy	10 MeV
Extraction energy	75 MeV
Accelerating voltage	5 MV
Number of orbits	13
Magnetic field (sector I/II)	0.51/0.60 T
Air gap (sector I/II)	20/17 mm

2 ELECTRON-OPTICAL DESIGN

The combination of two-sector profiled bending magnets and their rotation in the median plane offers an electron-optical system with inherent focusing at three edges of each magnet. For the design of the bending magnets, we have maximized the transverse acceptances with respect to the two degrees of freedom, offered by the choice of the two-sector profile. To calculate the transverse acceptances, the magnetic field has been modeled by sections with uniform magnetic field (hard-edge approximation) and the particle trajectories have been calculated from a sequence of first-order transfer matrices. The effect of the fringing fields on the vertical plane motion has been modeled by an extra defocusing force in the vertical plane. The strength of this extra force has been calculated from the magnetic field distribution in the median plane [5]. Furthermore, the effect of the cavity on the transverse motions has been incorporated by using the transfer matrix as given by *e.g.* ref.[6]. The specific magnetic field distribution in case of the microtron bending magnets has been obtained by applying the technique of conformal mapping [7, 8]. As a result of these model calculations, we have chosen a suitable magnet pole profile [8].

The thus obtained magnet pole profile has been realized and magnetic field measurements using a Hall probe have been done. Then, calculations with the code COSY INFINITY [1] have been carried out, where the measured magnetic field maps have been used as input. The resulting first-order matrix elements have been used to calculate the transverse acceptances at injection. These calculations yield a horizontal acceptance of about 40 mm-mrad and a vertical acceptance of about 55 mm-mrad at injection (see Figure 2). The aperture is taken to be 10 mm.

Besides the acceptances, we have also calculated the tunes, for each turn separately. The horizontal tunes vary from 1.2 at 15 MeV to 1.1 at 70 MeV. The vertical tunes vary from 0.4 at 15 MeV to 0.3 at 70 MeV. To illustrate

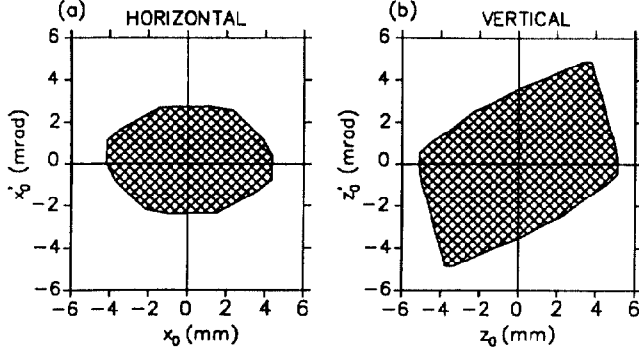


Figure 2: (a) Horizontal and (b) vertical acceptances at injection as obtained from particle tracking through the measured magnetic field maps.

the action of the electron-optical system, we have plotted some trajectories from injection to extraction in the horizontal plane (Figure 3a,b) and in the vertical plane (Figure 4a,b) for a parallel beam and a divergent beam, respectively. These results have been confirmed by numerical integration of the leading equations of motion, where the measured magnetic field maps in the median plane have been used as input [8].

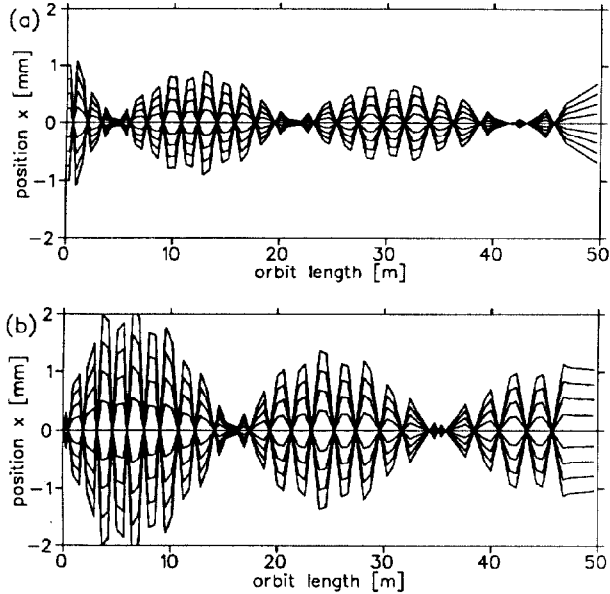


Figure 3: Trajectories in the horizontal plane for (a) a parallel beam and (b) a divergent beam as obtained from COSY INFINITY calculations.

From these figures, we see that the beam dimensions during the acceleration process are of the same order of magnitude as the beam dimensions at injection. This is due to the presence of strong focusing, which is obtained by proper shaping of the magnet poles.

Another consequence of the strong focusing is that the sensitivity of the trajectories for misalignments of the

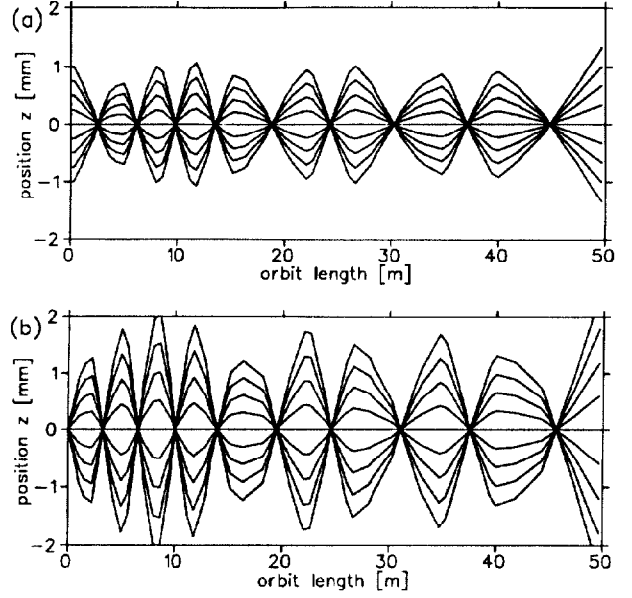


Figure 4: Trajectories in the vertical plane for (a) a parallel beam and (b) a divergent beam as obtained from COSY INFINITY calculations.

bending magnets is substantially reduced with respect to weak focusing microtrons. Numerical calculations [8] have shown that the alignment tolerances can be met by alignment of the bending magnets.

3 HIGHER-ORDER EFFECTS

In the analysis so far, we have neglected the effect of higher-order terms on the particle trajectories. In order to determine to what extent the above given acceptances are an adequate representation of the electron-optical system, we have calculated the acceptances for the case that higher-order terms are taken into account. To compare the first-order calculations with higher-order calculations, we define the acceptance \mathcal{A} to be the volume

$$\mathcal{A} = \iiint \int dx_0 dz_0 dx'_0 dz'_0, \quad (1)$$

where

$$\{(x_0, z_0, x'_0, z'_0) \mid |x(s)| \leq R \wedge |z(s)| \leq R, \forall s\}, \quad (2)$$

and

$$x = \sum_{\kappa, \lambda, \mu, \nu} (x | x_0^\kappa z_0^\lambda x_0'^\mu z_0'^\nu) x_0^\kappa z_0^\lambda x_0'^\mu z_0'^\nu, \quad (3)$$

$$z = \sum_{\kappa, \lambda, \mu, \nu} (z | x_0^\kappa z_0^\lambda x_0'^\mu z_0'^\nu) x_0^\kappa z_0^\lambda x_0'^\mu z_0'^\nu. \quad (4)$$

Here, the half-aperture R is taken to be 5 mm. The first-order acceptance \mathcal{A}^1 is obtained by letting $\kappa + \mu = 1$, $\lambda = \nu = 0$ in Eq.(3) and $\kappa = \mu = 0$, $\lambda + \nu = 1$ in Eq.(4) where $\kappa, \lambda, \mu, \nu \in \{0, 1\}$. The second-order acceptance \mathcal{A}^2 is obtained by letting $\kappa + \lambda + \mu + \nu = 2$, $\kappa, \lambda, \mu, \nu \in \{0, 1, 2\}$

The coefficients $(x|x_0^\kappa z_0^\lambda x_0^\mu z_0^\nu)$ and $(z|x_0^\kappa z_0^\lambda x_0^\mu z_0^\nu)$ in case of the microtron have been obtained from calculations with the code COSY INFINITY. As an illustration, we have plotted in Figure 5 the resulting all non-zero second-order coefficients after successive cavity passages at a position, directly at the end of the cavity. The end of the cavity is taken as reference since the cavity aperture is the main acceptance limitation. Here, the measured magnetic field maps have been used as input. The values of the coefficients $(x|x_0^\kappa z_0^\lambda x_0^\mu z_0^\nu)$ are typically between -400 and 400, whereas the values of the coefficients $(z|x_0^\kappa z_0^\lambda x_0^\mu z_0^\nu)$ are typically between -200 and 200. Realizing that the permissible positions x_0 , z_0 and divergences x_0' and z_0' are a few millimetres and milliradians, respectively, (see Figure 2 we see that, due to second-order effects, the horizontal beam size is increased typically 2 mm and the vertical beam size is increased typically 1 mm. Since we are

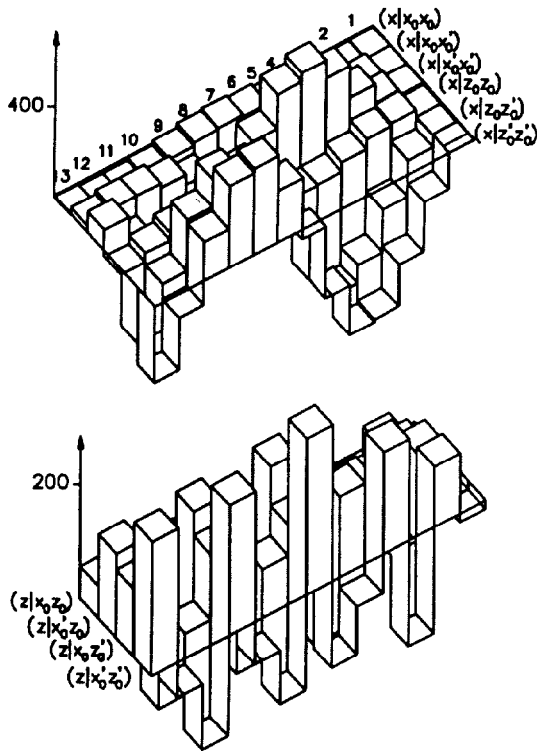


Figure 5: The values of the non-zero second-order coefficients as obtained from COSY INFINITY calculations after successive cavity passages at a position, directly at the end of the cavity.

interested in the effect of higher-order effects on the transverse acceptances, we have calculated the acceptance as defined in Eq.(1) for the case that only first-order terms have been taken into account, and for the case that also second-order terms have been taken into account (third- and higher-order terms can be neglected since they give no significant contribution to the acceptances). The ratio $\mathcal{A}^2/\mathcal{A}^1$ of the first- and second-order acceptances after successive cavity passages are given in Table 2.

Table 2: Second-order acceptance, relative to the first-order acceptance after successive cavity passages.

	1	2	3	4	5	6-13
$\mathcal{A}^2/\mathcal{A}^1$ (hor.)	1.00	1.00	1.00	1.00	0.99	0.99
$\mathcal{A}^2/\mathcal{A}^1$ (vert.)	0.99	0.97	0.95	0.94	0.93	0.92

First of all, we see that the forming of the acceptances takes place typically in the first few orbits. Furthermore, we see that the decrease of horizontal acceptance due to second-order effects is negligible, whereas the decrease of the vertical acceptance is only 8%. This means that, although the transverse beam sizes will increase 0.5-2 mm, higher-order effects are no point of concern as far as the transverse acceptances are concerned.

4 CONCLUSIONS

In this paper, we have described the electron-optical properties of the 75 MeV Eindhoven race-track microtron. The electron-optical design, and the resulting technical design, of the microtron is based on model calculations, where only first-order effects have been taken into account. Calculations where also higher-order effects have been taken into account have shown that, although the transverse acceptances decrease slightly, the resulting acceptances are still sufficient to match the emittance of the linac-microtron beam transport line.

5 ACKNOWLEDGEMENT

The authors like to thank M. Berz and K. Fuchi at National Superconducting Cyclotron Laboratory, Michigan, USA, for their assistance and for their support of the code COSY INFINITY.

6 REFERENCES

- [1] M. Berz - *COSY INFINITY version 6 user's guide and reference manual*, Michigan State University, USA (1993).
- [2] G.A. Webers *et al.* - *Optical design of the 75 MeV Eindhoven Race-track microtron*, Proc. Part. Acc. Conf. Washington D.C. (1993) pp.2062-2064.
- [3] B. Xi *et al.* - *Design study of the storage ring EUTERPE*, Nucl. Instr. and Meth. B68 (1992) pp.101-104.
- [4] J.L. Delhez *et al.* - *Electron beam focusing in a race-track microtron by means of rotated two-sector magnets*, Nucl. Instr. and Meth. B68 (1992) pp.96-100.
- [5] K.L. Brown - *A first and second order matrix theory for the design of beam transport systems and charged spectrometers*, Advances Part. Phys. 1 (1967) pp.71-134.
- [6] R.E. Rand - *Recirculating electron accelerators*, Harwood academic publ. (1984).
- [7] G.A. Webers *et al.* - *Fringe field calculations for the inhomogeneous Twente Eindhoven microtron magnets*, Nucl. Instr. and Meth. B68 (1992) pp.83-86.
- [8] G.A. Webers - *Design of an electron-optical system for a 75 MeV Race-track microtron*, Ph.D. thesis, Eindhoven University Of Technology (1994).